

# Variation of the Great Auricular Nerve and Prediction of the Facial Nerve Trunk Size

Krist Kriengkraikasem, MD\*  
Kritsada Kowitwibool, MD\*  
Malee Chanpoo, PhD†

**Background:** This study aimed to reveal the anatomical variation in the great auricular nerve (GAN) and the correlation between the size of the GAN and the facial nerve trunk (FNT), so as to aid surgeons to perform safe facelift surgery and parotidectomy.

**Methods:** Sixteen human cadavers were studied on 16 left and 15 right facial sides. The GAN's branching patterns, location, and the mean width of the GAN and FNT were measured.

**Results:** The average distance where the nerve emerged from under the sternocleidomastoid muscle was  $87.61 \pm 12.13$  mm when measured perpendicular to the Frankfort horizontal plane. The branching pattern of the GAN could be classified into 5 types of which the most common was type 3 (30.77%), where the GAN divided into the anterior (superficial) and posterior branches, and then the deep branch originated from the posterior branch of the GAN. The mean width of the GAN and FNT from all the dissections was  $3.26 \pm 0.67$  mm and  $3.36 \pm 0.71$  mm, respectively. There was a significant correlation between the width of the nerves on both facial sides (right:  $r = 0.740$ ,  $P = 0.002$ ; left:  $r = 0.839$ ,  $P < 0.001$ ).

**Conclusions:** This study revealed the anatomical variation and the width of the GAN, which can strongly predict the width of the FNT. This should be taken into consideration during facelift surgery and parotidectomy, especially in patients with a small GAN to prevent iatrogenic injury to the small FNT. (*Plast Reconstr Surg Glob Open* 2018;6:e2000; doi: 10.1097/GOX.0000000000002000; Published online 17 December 2018.)

## INTRODUCTION

During parotidectomy and facelift surgery, the incisions are usually made with a modified Blair incision and facelift incision.<sup>1-4</sup> Surgical exposures are initiated via elevation of the lateral facial and neck skin. Two important sensory and motor nerves are located in this region: the great auricular nerve (GAN) and the facial nerve (FN), respectively, which are found superficial to the deep surgical plane.<sup>1</sup>

The GAN originates from the cervical plexus at levels of C2 and C3, pierces the investing fascia at the posterior border of the sternocleidomastoid muscle (SCM), approximately halfway between the mastoid process and the sternal notch. It ascends toward the ear and on reaching the parotid gland, it divides into anterior and posterior branches to contribute sensory fibers to the skin overlying the parotid area, lower aspect of the pinna and angle of the mandible.<sup>5-10</sup> Injury to the GAN during facelift surgery, which has estimated incidence from 0% to 6%,<sup>11-21</sup> can occur while skin flaps are being undermined.<sup>7</sup> Although not as significant as motor nerve injury, iatrogenic injury of the GAN can have long-term sequelae.<sup>11</sup>

The FN is commonly referred to as the nerve of facial expression.<sup>22,23</sup> It exits the skull base by passing through the stylomastoid foramen and then runs an-

From the \*Division of Facial Plastic and Reconstructive Surgery, Department of Otolaryngology, Faculty of Medicine, Chulalongkorn University, Bangkok, Thailand; and †Department of Anatomy, Phramongkutklao College of Medicine, Royal Thai Army, Bangkok, Thailand.

Received for publication August 23, 2018; accepted September 14, 2018.

Copyright © 2018 The Authors. Published by Wolters Kluwer Health, Inc. on behalf of The American Society of Plastic Surgeons. This is an open-access article distributed under the terms of the Creative Commons Attribution-Non Commercial-No Derivatives License 4.0 (CCBY-NC-ND), where it is permissible to download and share the work provided it is properly cited. The work cannot be changed in any way or used commercially without permission from the journal.

DOI: 10.1097/GOX.0000000000002000

**Disclosure:** The authors have no financial interest to declare in relation to the content of this article. The Article Processing Charge was 50% waived at the discretion of the Editor-in-Chief.

Supplemental digital content is available for this article. Clickable URL citations appear in the text.

teriorly within the parenchyma of the parotid gland, crosses the external carotid artery, and divides into 2 main divisions at the posterior border of the ramus of the mandible, an upper (temporofacial) division and a lower (cervicofacial) division.<sup>1,22-25</sup> In general, 2 basic surgical approaches have been used to identify and preserve the FN trunk (FNT) during surgery of the parotid gland. One method is to identify the FNT by dissecting the nerve from proximal to distal ends. The other is retrograde identification by dissecting the peripheral nerve branches after bifurcation of the FNT. The use of the former technique is generally believed to be safer and more reliable.<sup>1,24</sup>

In current practice, wide ranges of landmarks and nerve monitoring are used to identify the FNT<sup>23,24,26-33</sup> without any principle in terms of the size prediction of the FNT that the surgeon will encounter. However, only limited clinical experience and 1 pilot study implied a relationship between the width of the GAN and the size of the main FNT.<sup>34-37</sup> The purpose of this study was, therefore, to reveal the anatomical variation (location and branching) of the GAN and to provide a size prediction of the FNT to aid surgeons for safe facelift surgery and parotidectomy.

### MATERIALS AND METHODS

This was a collaborative study between the Division of Facial Plastic and Reconstructive Surgery, Department of Otolaryngology, Faculty of Medicine, Chulalongkorn University and the Department of Anatomy, Phramongkutklao College of Medicine, Royal Thai Army. The required sample size calculation, based on Colbert S et al.<sup>37</sup> that the mean width of the GAN and FNT was  $2.75 \pm 0.53$  mm and  $2.83 \pm 0.54$  mm, respectively, was calculated to be about 15 according to the formula:

$$\alpha = 0.05 \text{ (two-sided test)} \quad Z_{0.025} = 1.96$$

$$n_{GAN} = \frac{Z_{\alpha/2}^2 \sigma^2}{d^2}$$

$$= \frac{(1.96)^2 (0.53)^2}{(0.10 \times 2.75)^2}$$

$$= 14.27$$

$$n \approx 15$$

$$n_{FNT} = \frac{Z_{\alpha/2}^2 \sigma^2}{d^2}$$

$$= \frac{(1.96)^2 (0.54)^2}{(0.10 \times 2.83)^2}$$

$$= 13.99$$

$$n \approx 14$$

Sixteen intact cadavers were obtained in conjunction with all the cadavers given to second-year medical students in Department of Anatomy, Phramongkutklao College of Medicine, Royal Thai Army. Both sides of the face and neck were dissected to explore the GAN and the FNT

with all dissections and measurements completed by the authors and a single observer, respectively, before the student dissection of the face and neck. There was institutional approval for this study. The precise course of the GAN and the extent of its branching were established by careful dissection and then identifying the FNT by dissecting the nerve from proximal to distal ends using various anatomic landmarks.<sup>1,23,24,26,28,30</sup>

The study consisted of 3 investigations concerning the anatomical variation of the GAN and prediction of the FNT size. The GAN location at its emergence from underneath the sternocleidomastoid muscle was measured in the first investigation. We measured the distance where the nerve emerged perpendicular to the Frankfort horizontal plane (Fig. 1). In the second investigation, the branching pattern of the anterior, posterior, superficial, and deep branches of the GAN were recorded and classified into 5 types. Lastly, to assess the correlation between the sizes of the GAN and FNT, the widest dimensions of the GAN before bifurcating into the anterior and posterior branches (Figs. 2A and 3A) and the main FNT before bifurcating into the upper (temporofacial) and lower (cervicofacial) branches were measured (Figs. 2B and 3B). All measurements were made by a single observer, an otolaryngologist, using digital calipers: Mitutoyo No.500-196-20. CD-6" CSX (Made in Japan) capable of measuring to 0.01 mm. Precise measurements were achieved by intensive training on the quantification technique in advance. Ten square toy blocks were randomly given to the observer with an interval of 2 days to 2 weeks between sessions. An intraclass correlation above 0.96 was reached before the initiation of study. Each measurement was performed with the calipers reset to zero every time. The mean, SD, and range for each of the measurements were determined. Pearson's product moment correlations coefficients were calculated to assess any association between the diameters of the GAN and the FNT. The agreement was analyzed using the model described by Bland and Altman. Data were analyzed using Statistical Package for Social Science (version 22). A 2-sided *P* value of <0.05 was regarded as statistically significant.



**Fig. 1.** Location of the GAN at its emergence from underneath the SCM.

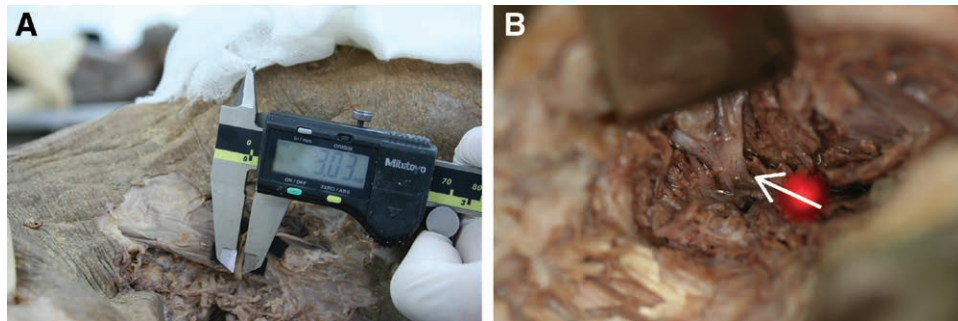


**Fig. 2.** A, The width of the GAN before bifurcating into the anterior and posterior branches was measured. B, Arrow indicates the main FNT before bifurcating into the upper (temporofacial) and lower (cervicofacial) branches.

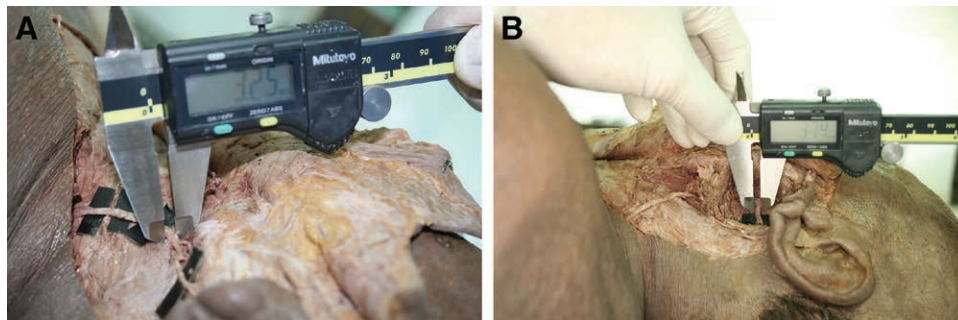


**Fig. 3.** A, The GAN ascending toward the parotid gland was measured before the bifurcation. B, The main trunk of the FN was measured with a digital caliper to 0.01 mm.

### RESULTS

The 16 cadavers (11 males, 5 females) examined had an age range between 49 and 94 years old. We recorded the results from both facial sides (16 left but only 15 right) and then further divided the data into the left and right facial sides in case of asymmetrical differences.

The distance where the GAN emerged from under the sternocleidomastoid muscle was ranged from 69.32 to 113.69 mm, with an average distance of  $87.61 \pm 12.13$  mm when measured perpendicular to the Frankfort horizontal plane (Fig. 1).

In the second investigation, even with careful dissection, we could complete the dissection to identify all the branches of the GAN in only 26 sides, since 5 sides (16.13%) were excluded after being accidentally cut while elevating the skin flap. In these 26 cases, the GAN divided into 4 branches (anterior, posterior, superficial, and deep branches) in its course on the sternocleidomastoid muscle. The superficial branch distributed to the skin and surface of the parotid gland, while the deep branch entered the parenchyma of the parotid gland. The branching patterns could be subdivided into 5 main categories (see figure, Supplemental Digital Content 1, <http://links.lww.com/PRSGO/A909>, which displays photographs and diagrams showing the five branching patterns (types 1–5 in A–E, respectively) of the GAN). In type 1 (Supplemental Digital Content 1), found in 5 sides (19.23%), the GAN divided into the anterior and posterior branches, and then the anterior branch bifurcated into the superficial and deep branches. In type 2 (Supplemental Digital Content 1),

**Table 1. Size (Mean, SD and Range) of the Right and Left Facial Side GAN and FN in Millimeter**

Structure	Mean	SD	Minimum	Maximum
Right GAN	3.17	0.68	2.00	4.26
Left GAN	3.35	0.68	2.14	4.57
Right FN	3.27	0.75	2.03	4.88
Left FN	3.44	0.68	2.20	4.81

found in 3 sides (11.54%), a trifurcation of the GAN, the posterior branch and the superficial and deep branches of the anterior branch was evident. Type 3 (Supplemental Digital Content 1), found in 8 sides (30.77%), was the most common pattern, where the deep branch originated from the posterior branch of the GAN and the anterior branch ran superficial distributed to the skin and surface of the parotid gland. In Type 4 (Supplemental Digital Content 1), found in 7 sides (26.92%), the superficial branch originated from the posterior branch of the GAN and the anterior branch ran deep into the parenchyma of the parotid gland. Lastly, in type 5 (Supplemental Digital Content 1), found in 3 sides (11.54%), the GAN had already bifurcated into the anterior and posterior branches by the time it had emerged onto the sternocleidomastoid muscle through the investing fascia.

Lastly, to assess the correlation between the GAN and the FNT, the results and the side of dissection was recorded. The mean width of the GAN and the FNT from all the dissections was  $3.26 \pm 0.67$  mm and  $3.36 \pm 0.71$  mm, respectively. The mean width of each nerve from both sides are shown in Table 1.

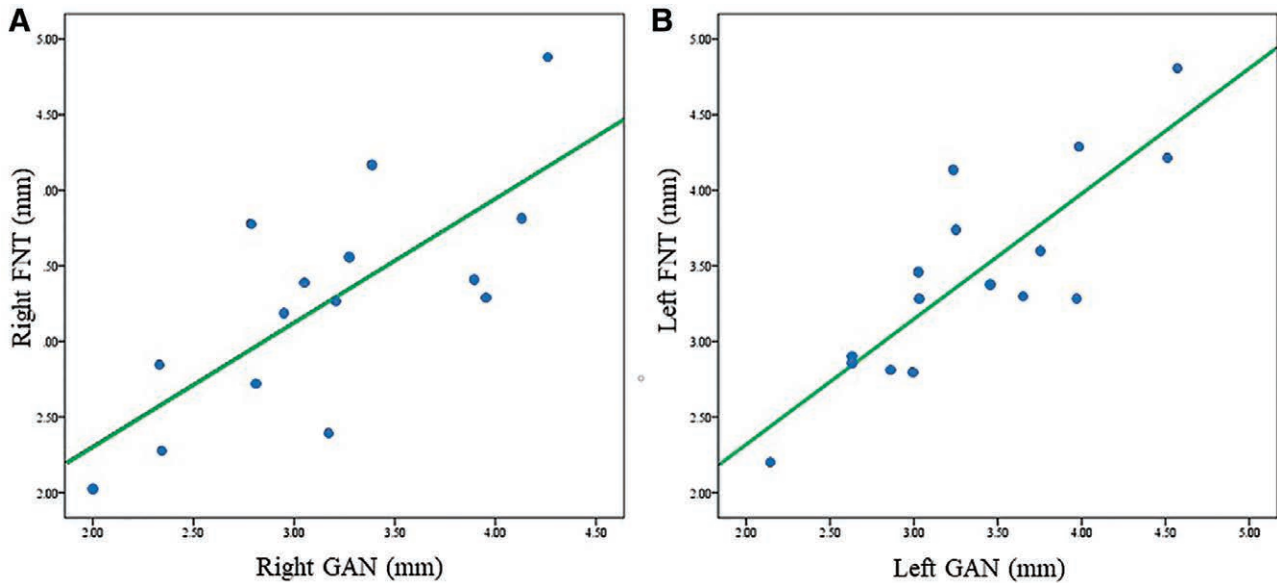


**Fig. 4.** Correlation between the diameter of the GAN and FNT for the right ( $r = 0.740, P = 0.002$ ; A) and left ( $r = 0.839, P < 0.001$ ; B) facial side.

**Table 2. Regression Models and Fit Statistics to Predict the FNT Diameter from that of the GAN**

Variables	Optimum		
	Right Facial Side Model Coefficients	Optimum Left Facial Side Model	Optimum Mean Model
GAN (R)	0.82	—	—
GAN (L)	—	0.831	—
Mean GAN	—	—	0.893
95% CI for coefficient	0.374–1.266	0.522–1.139	0.616–1.171
R <sup>2</sup> /adjusted R <sup>2</sup>	0.548/0.513	0.704/0.683	0.788/0.772
Standard error of estimate	0.522	0.380	0.306

Dependent variables for the models are the FN measurements (right, left, and mean of both facial sides).

Pearson’s product moment correlations coefficients were calculated to assess any association between the diameters of the GAN and the FNT. A strong positive correlation between the diameters of the 2 nerves was found for both the right ( $r = 0.740; P = 0.002$ ) and left ( $r = 0.839; P < 0.001$ ) facial sides (Fig. 4). We confirmed the relationship between the FNT size and the GAN diameter with regression analysis for each facial side and the mean from both sides (Table 2).

Bland-Altman plots (Fig. 5) and 95% confidence interval (CI) for limits of agreement (Table 3) were used to evaluate the agreement among the 2 different values, and the diagrams indicate that the diameter of the GAN was very similar to that of the FNT and can be used interchangeably.

## DISCUSSION

The impact of GAN sacrifice morbidity on the patient’s quality of life is tolerable and improves during the first postoperative year. However, GAN morbidity may be bothersome enough to warrant efforts to preserve the branch of the GAN when possible.<sup>38,39</sup> In our study, the location where the GAN emerged from the posterior border

of the sternocleidomastoid muscle (Erb’s point)<sup>5,6</sup> was  $87.61 \pm 12.13$  mm below the Frankfort horizontal plane, the most consistent reference. In contrast to other studies, the GAN was found approximately 1 cm posterior to the external jugular vein<sup>7,40</sup> and was reported to emerge from under the sternocleidomastoid muscle, as measured from the bony external auditory canal at either  $6.5 \pm 0.9$  cm or  $9.8 \pm 1.2$  cm.<sup>7,11</sup> Due to the delicate GAN branching pattern, 5 sides (16.1%) were accidentally cut while elevating the skin flap and so were excluded from the analysis. We feel that this unintentional cut is inevitable, but note that its incidence (16.1%) is less than that for the postoperative hypesthesia of the ear from parotid gland surgery, which has an estimated incidence of from 26% to 59%.<sup>41–44</sup> The patterns of branching of the GAN was previously described by Ozturk et al.,<sup>11</sup> where 4 types of branching patterns of the nerve were identified: branching at the superior third of the SCM (type 1), branching at the mid-third of the SCM (type 2), branching at the inferior third of the SCM (type 3), and no branching (type 4). The most common branching pattern was type 1 (53.8%), followed by type 3 (26.9%), type 4 (15.4%), and type 2 (3.8%). However, this was based upon only the anterior and posterior branches. In contrast, in this study, we included the superficial and deep branches as well and so could classify 5 types of branching pattern. The most common branching pattern was type 3 (30.77%), where the deep branch originated from the posterior branch of the GAN and the anterior branch ran superficial distributed to the skin and surface of the parotid gland. This is similar to that previously reported,<sup>45</sup> where the most frequently observed pattern (28%) was where the deep branch originated from the posterior branch of the GAN. These confirm the difference to Gray’s Anatomy<sup>9</sup> that described the GAN as being divided into the anterior and posterior branches, and then the anterior branch bifurcated into the superficial

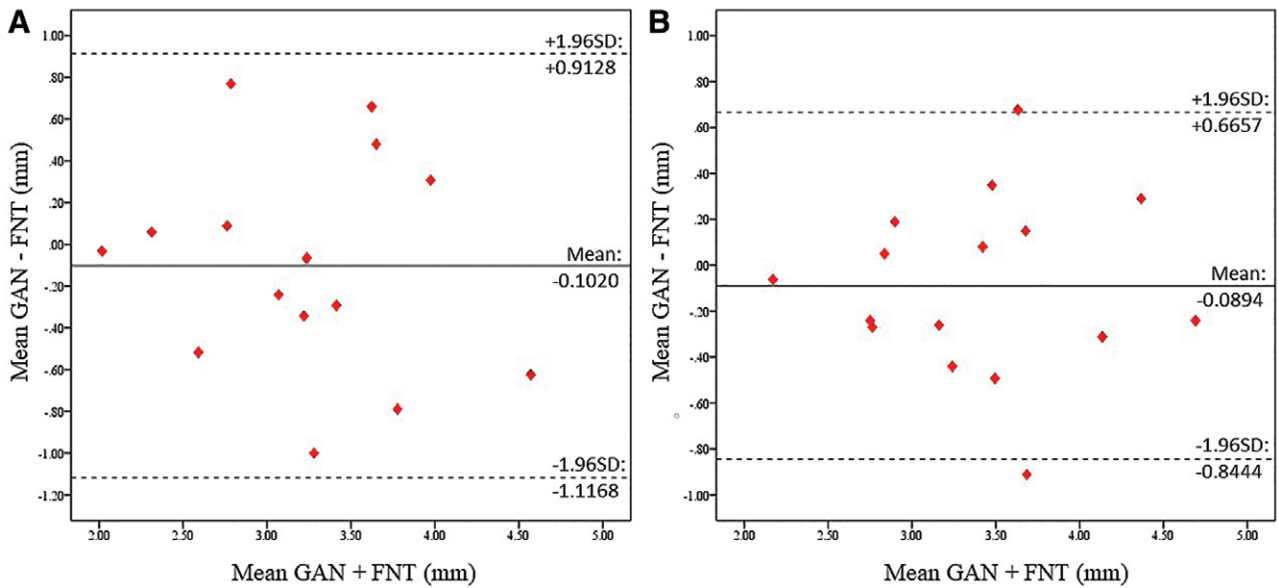


**Fig. 5.** Bland and Altman plot of the absolute limits of agreement between the size of the GAN and FNT for the (A) right and (B) left facial side.

**Table 3. 95% CI for Limits of Agreement between the Diameter of GAN and FNT**

Facial Side	Bias	95% Lower Limit	95% Upper Limit
Right side (n = 15)	-0.1020	-1.1168	0.9128
Left side (n = 16)	-0.0894	-0.8444	0.6657

and deep branches, which matches our type 1 branching pattern and accounts for only 19.23% of the patterns seen. The least common patterns were the trifurcation (type 2; 11.54%) and the bifurcation before emerging on to the sternocleidomastoid muscle (type 5; 11.54%).

From individual clinical experiences, a small and delicate GAN corresponds to subsequently finding a small and delicate FN. It would appear the converse also holds true in that a robust GAN is correlated with a similarly robust FNT.<sup>34-36</sup> To the best of our knowledge, this study is the first attempt to confirm the initial pilot study<sup>37</sup> by using a very delicate measurement capable of measuring to 0.01 mm (Figs. 2, 3). The results confirmed that the width of the FNT can be predicted from the width of the GAN before its bifurcation.

However, this study has some possible limitations. In addition to limited ethnical divergence, we studied cadavers, which can be associated with the shrinkage of soft tissue.<sup>46,47</sup>

**Krist Kriengkraikasem, MD**

Division of Facial Plastic and Reconstructive Surgery  
 Department of Otolaryngology  
 Faculty of Medicine  
 Chulalongkorn University – 1873  
 Department of Otolaryngology Head and Neck Surgery  
 King Chulalongkorn Memorial Hospital  
 The Thai Red Cross Society Rama IV Rd.  
 Pathumwan Bangkok 10330, Thailand  
 E-mail: Krist\_smile@hotmail.com

**REFERENCES**

- Montgomery WW. Montgomery. *Surgery of the Upper Respiratory System*. 2nd ed. Philadelphia, Pa.: Lea & Febiger; 1989.
- Wormald R, Donnelly M, Timon C. ‘Minor’ morbidity after parotid surgery via the modified Blair incision. *J Plast Reconstr Aesthet Surg*. 2009;62:1008–1011.
- Beahrs OH. The surgical anatomy and technique of parotidectomy. *Surg Clin North Am*. 1977;57:477–493.
- Lohuis PJ, Tan ML, Bonte K, et al. Superficial parotidectomy via facelift incision. *Ann Otol Rhinol Laryngol*. 2009;118:276–280.
- Ginsberg LE, Eicher SA. Great auricular nerve: anatomy and imaging in a case of perineural tumor spread. *AJNR Am J Neuroradiol*. 2000;21:568–571.
- Leung MK, Dieu T, Cleland H. Surgical approach to the accessory nerve in the posterior triangle of the neck. *Plast Reconstr Surg*. 2004;113:2067–2070.
- Lefkowitz T, Hazani R, Chowdhry S, et al. Anatomical landmarks to avoid injury to the great auricular nerve during rhytidectomy. *Aesthet Surg J*. 2013;33:19–23.
- McKinney P, Katrana DJ. Prevention of injury to the great auricular nerve during rhytidectomy. *Plast Reconstr Surg*. 1980;66:675–679.
- Standring S. *Gray’s Anatomy: The Anatomical Basis of Clinical Practice*. 41st ed. Edinburgh, Scotland: Churchill Livingstone; 2015;29: 442–474.e1.
- Peuker ET, Filler TJ. The nerve supply of the human auricle. *Clin Anat*. 2002;15:35–37.
- Ozturk CN, Ozturk C, Huettner F, et al. A failsafe method to avoid injury to the great auricular nerve. *Aesthet Surg J*. 2014;34:16–21.
- Rees TD, Aston SJ. Complications of rhytidectomy. *Clin Plast Surg*. 1978;5:109–119.
- Waterhouse N, Vesely M, Bulstrode NW. Modified lateral SMASectomy. *Plast Reconstr Surg*. 2007;119:1021–1028.
- Hopping SB, Joshi AS, Tanna N, et al. Volumetric facelift: evaluation of rhytidectomy with alloplastic augmentation. *Ann Otol Rhinol Laryngol*. 2010;119:174–180.
- Matarasso A, Elkwood A, Rankin M, et al. National plastic surgery survey: face lift techniques and complications. *Plast Reconstr Surg*. 2000;106:1185–1196.

16. Berry MG, Davies D. Platysma-SMAS plication facelift. *J Plast Reconstr Aesthet Surg*. 2010;63:793–800.
17. Marchac D, Sándor G. Face lifts and sprayed fibrin glue: an outcome analysis of 200 patients. *Br J Plast Surg*. 1994;47:306–309.
18. Lawson W, Naidu RK. The male facelift: an analysis of 115 cases. *Arch Otolaryngol Head Neck Surg*. 1993;119:535–541.
19. Scarborough D, Bisaccia E. The Webster-type face and neck lift: an extensive cervico-facial rhytidectomy employing a minimally invasive technique. *Dermatol Surg*. 2001;27:747–755.
20. Matarasso A, Wallach SG, Difrancesco L, et al. Age-based comparisons of patients undergoing secondary rhytidectomy. *Aesthetic Surg J*. 2002;22:526–530.
21. Stuzin JM. MOC-PSSM CME article: face lifting. *Plast Reconstr Surg*. 2008;121:1–19.
22. Monkhouse S. *Cranial Nerves: Functional Anatomy*. New York, United States of America: Cambridge University Press; 2005.
23. Pather N, Osman M. Landmarks of the facial nerve: implications for parotidectomy. *Surg Radiol Anat*. 2006;28:170–175.
24. Nishida M, Matsuura H. A landmark for facial nerve identification during parotid surgery. *J Oral Maxillofac Surg*. 1993;51:451–453.
25. Janfaza P, Cheney ML. Superficial structures of the face, head, and parotid region. In Janfaza P, Nadol JB, Galla R, Fabian RL, Montgomery WW, eds. *Surgical Anatomy of the Head and Neck*. Philadelphia, Pa.: Lippincott William & Wilkins; 2001: 1–48.
26. Ji YD, Donoff RB, Peacock ZS, et al. Surgical landmarks to locating the main trunk of the facial nerve in parotid surgery: a systematic review. *J Oral Maxillofac Surg*. 2018;76(2):438–443.
27. Kwak HH, Park HD, Youn KH, et al. Branching patterns of the facial nerve and its communication with the auriculotemporal nerve. *Surg Radiol Anat*. 2004;26:494–500.
28. Bernstein L, Nelson RH. Surgical anatomy of the extraparotid distribution of the facial nerve. *Arch Otolaryngol*. 1984;110:177–183.
29. Katz AD, Catalano P. The clinical significance of the various anatomic branches of the facial nerve. Report of 100 patients. *Arch Otolaryngol Head Neck Surg*. 1987;113:959–962.
30. Roostaeian J, Rohrich RJ, Stuzin JM. Anatomical considerations to prevent facial nerve injury. *Plast Reconstr Surg*. 2015;135:1318–1327.
31. Dulguerov P, Marchal F, Lehmann W. Postparotidectomy facial nerve paralysis: possible etiologic factors and results with routine facial nerve monitoring. *Laryngoscope*. 1999;109:754–762.
32. Witt RL. Facial nerve monitoring in parotid surgery: the standard of care? *Otolaryngol Head Neck Surg*. 1998;119:468–470.
33. Terrell JE, Kileny PR, Yian C, et al. Clinical outcome of continuous facial nerve monitoring during primary parotidectomy. *Arch Otolaryngol Head Neck Surg*. 1997;123:1081–1087.
34. Whear NM, Lopes V. The great auricular and the facial nerve: is there a correlation between the diameter of these nerves? *Br J Oral Maxillofac Surg*. 2001;39:162–163.
35. Rayatt S. Re: Whear NM, and Lopes V. The great auricular nerve and the facial nerve. *Br J Oral Maxillofac Surg* 2001; 39: 162-163. *Br J Oral Maxillofac Surg*. 2001;39:486.
36. Ezsias A. The great auricular and the facial nerve: is there a correlation between the diameter of these nerves?—observations. *Br J Oral Maxillofac Surg*. 2002;40:348.
37. Colbert S, Parry DA, Hale B, et al. Does the great auricular nerve predict the size of the main trunk of the facial nerve? A clinical and cadaveric study. *Br J Oral Maxillofac Surg*. 2014;52:230–235.
38. Ryan WR, Fee WE Jr. Great auricular nerve morbidity after nerve sacrifice during parotidectomy. *Arch Otolaryngol Head Neck Surg*. 2006;132:642–649.
39. Brown JS, Ord RA. Preserving the great auricular nerve in parotid surgery. *Br J Oral Maxillofac Surg*. 1989;27:459–466.
40. Murphy R, Dziegielewski P, O’Connell D, et al. The great auricular nerve: an anatomic and surgical study. *J Otolaryngol Head Neck Surg*. 2012;41:S75–S77.
41. Biswas AK, Akhtar N, Debnath TK, et al. Complications of parotid Surgery – A study of 30 cases. *Bangladesh J Otorhinolaryngol*. 2015 Apr;21(1):23–27.
42. Linder TE, Huber A, Schmid S. Frey’s syndrome after parotidectomy: A retrospective and prospective analysis. *Laryngoscope*. 1997 Nov;107(11):1496–1501.
43. Koch M, Zenk J, Iro H. Long-term results of morbidity after parotid gland surgery in benign disease. *Laryngoscope*. 2010 Apr;120(4):724–730.
44. Correia M, Noronha FP, Audi P. Superficial parotidectomy an excellent procedure in the management of benign parotid tumors – outcome of various complications and tumor recurrence. *Med J DY Patil Univ*. 2016 Sep;9(5):600–604.
45. Yang HM, Kim HJ, Hu KS. Anatomic and histological study of great auricular nerve and its clinical implication. *J Plast Reconstr Aesthet Surg*. 2015 Feb 28;68(2):230–236.
46. Chen CH, Hsu MY, Jiang RS, et al. Shrinkage of head and neck cancer specimens after formalin fixation. *J Chin Med Assoc*. 2012;75:109–113.
47. Kerns MJ, Darst MA, Oslan TG, et al. Shrinkage of cutaneous specimens: formalin or other factors involved? *J Cutan Pathol*. 2008;35:1093–1096.